UGC 12732: A DISK GALAXY LACKING HIGH-VELOCITY CLOUDS

ERIC SCHULMAN[1]

National Radio Astronomy Observatory, 520 Edgemont Road, Charlottesville, Virginia 22903-2475
Electronic mail: eschulma@nrao.edu

ELIAS BRINKS[2]

National Radio Astronomy Observatory, P.O. Box O, Socorro, New Mexico 87801-0387
Electronic mail: ebrinks@nrao.edu

JOEL N. BREGMAN

Department of Astronomy, University of Michigan, Ann Arbor, Michigan 48109-1090
Electronic mail: jbregman@umich.edu

MORTON S. ROBERTS

National Radio Astronomy Observatory, 520 Edgemont Road, Charlottesville, Virginia 22903-2475
Electronic mail: mroberts@nrao.edu

ABSTRACT

We used the Very Large Array to obtain high-sensitivity 21 cm synthesis images of the disk galaxy UGC 12732. This object did not show high-velocity wings in Arecibo telescope spectra obtained to search for populations of high-velocity clouds in external galaxies. The VLA observations confirm the absence of high-velocity H I in UGC 12732: we set an upper limit of 2×10^7 $M_\odot$ for high-velocity material, consistent with the upper limit of 5×10^7 $M_\odot$ inferred from the Arecibo observations. The gas distribution perpendicular to the disk is successfully represented by a thin layer with a constant Gaussian velocity dispersion of $\sigma_v = 9$ km s^{-1}. UGC 12732 has a low star formation rate, which is consistent with previous findings that galaxies without active star formation lack high-velocity H I clouds. © *1997 American Astronomical Society.* [S0004-6256(97)02205-X]

1. INTRODUCTION

The high-velocity clouds of neutral hydrogen in our Galaxy dominate the kinetic energy of H I in non-circular motion and are an important though poorly understood component of Galactic gas. High-velocity clouds (HVCs) with $|v_{LSR}| > 100$ km s^{-1} cover approximately 18% of the sky to a limiting column density of 2 to 3×10^{18} cm^{-2} (Wakker 1991). The nature and origin of these HVCs are not well understood, in part because the uncertain distances to the clouds prevent accurate determinations of their masses, linear diameters, or densities. Wakker (1990) showed that it is possible to reproduce the observed distribution of most of the Galactic high-velocity clouds with two populations of gas: galactic fountain gas from superbubbles that breaks out of the Galactic disk, cools radiatively as it rises upward, and eventually recombines and returns to the disk ballistically (Shapiro & Field 1976; Bregman 1980), and Magellanic Stream material that is falling onto the Galaxy from the Magellanic Clouds (Murai & Fujimoto 1980). High-velocity clouds in the galactic fountain model have a characteristic distance of 10 to 20 kpc above the Galactic plane, while Magellanic Stream material has a characteristic distance of about 50 kpc (Wakker 1990). If these two processes are the dominant sources for Galactic HVCs, then high-velocity clouds are a disk-wide phenomenon that comprises about 10% of the neutral hydrogen in the Galaxy. However, if most high-velocity clouds are local then there may be relatively little mass in HVCs. To date there has been only one distance determination to a high-velocity cloud: HVC Complex M is at a distance of $1.7 < D < 5.0$ kpc (Danly *et al.* 1993). Lower limits to the distance of several other high-velocity cloud complexes have been reported: HVC Complex H has $D > 1.5$ kpc (Centurión *et al.* 1994), HVC Complex A has $D > 4$ (Wakker *et al.* 1996a), and HVC Complex C has $D > 2.5$ kpc (Wakker *et al.* 1996b). Because the distances almost all the HVCs in our Galaxy are unknown, further insight into the nature of high-velocity clouds can be obtained by finding and studying high-velocity gas in other galaxies and by investigating the differences between galaxies with and without HVCs.

A 21 cm survey of 14 nearly face-on disk galaxies using the Arecibo telescope[3] revealed that 70% of the galaxies have high-velocity wings beyond the double-horned H I pro-

---

TABLE 1. General information on UGC 12732.

Parameter	Value	Source
Morphological type	Sm:	Nilson (1973)
α (B1950) of optical center	$23^h\ 38^m\ 9^s1$	Dressel & Condon (1976)
δ (B1950) of optical center	$+25°\ 57'\ 30''$	Dressel & Condon (1976)
D_{25}	$3'0 \pm 0'2$	de Vaucouleurs *et al.* (1991)
Adopted distance	20 Mpc[a]	Schulman *et al.* (1994)
B	13.64 ± 0.02	Schulman (1995)
R	12.51 ± 0.02	Schulman (1995)
L_B	$3.3 \pm 0.7 \times 10^8\ L_\odot$[b]	Schulman (1995)
$L_{H\alpha}$	$1.5 \pm 0.5 \times 10^7\ L_\odot$[b]	Schulman (1995)
L_{FIR}	$7.8 \pm 3.6 \times 10^7\ L_\odot$	Schulman (1995)
Heliocentric systemic velocity	749 ± 2 km s^{-1}	This paper
Rotational velocity, v_{rot}	90 km s^{-1}	This paper
Inclination of inner disk	33°	This paper
PA of inner disk major axis	10–15°	This paper
Maximum H I radius at $N_{H\,I}=10^{19}$ cm^{-2}	$5'8 = 35$ kpc	This paper
Total H I linewidth (FWHM)	120 km s^{-1}	This paper
Total H I integrated flux density	82 Jy km s^{-1}	This paper
Total H I mass	$7.2 \times 10^9\ M_\odot$	This paper
Arecibo H I mass	$2.0 \times 10^9\ M_\odot$	Schulman *et al.* (1994)
"Corrected" Arecibo H I mass	$2.3 \times 10^9\ M_\odot$	Corrected as in Hewitt *et al.* (1983)
Total mass within the optical disk, M_{Tot}	$1.6 \times 10^{10}\ M_\odot$	$0.5\ D_{25} \times v_{rot}^2\ /\ G$
M_{Tot}/L_B	$7.3\ M_\odot/L_{\odot,B}$[c]	This paper
Arecibo H I mass to M_{Tot} ratio, "$M_{H\,I}/M_{Tot}$"	0.14	Calculated as in Roberts & Haynes (1994)

[a]Consistent with $H_0 = 50$ km s^{-1} Mpc^{-1}.
[b]Corrected for Galactic and internal extinction.
[c]Uncorrected for Galactic or internal extinction. $L_{\odot,B}=5\times10^{32}$ ergs s^{-1}.

file; these wings are the expected signature of HVCs in a disk galaxy (Schulman *et al.* 1994). The four galaxies without high-velocity wings have low star formation rates, as determined from optical and far-infrared observations (Schulman *et al.* 1994; Schulman 1995). These filled-aperture observations are very suggestive, but they require confirmation and do not in any case contain information on the spatial distribution of the high-velocity gas.

Very Large Array (VLA)[4] observations of NGC 5668, one of the galaxies with high-velocity wings, revealed more than $4 \times 10^8\ M_\odot$ of high-velocity neutral hydrogen, most of which is located primarily outside the optical disk of the galaxy and may be infalling material comparable to the Magellanic Stream in our own Galaxy (Schulman *et al.* 1996). About 40% of the high-velocity gas that was detected with Arecibo is located within the optical disk and may be halo gas produced by a galactic fountain. The VLA observations of NGC 5668 also reveal an increased H I velocity dispersion within the optical radius of the galaxy. Increased velocity dispersions have also been found within the optical disks of NGC 1058 (Dickey *et al.* 1990) and NGC 6946 (Kamphuis & Sancisi 1993; Boulanger & Viallefond 1992). Massive stars and young regions of star formation transmit energy to the gas via expanding H II regions, stellar winds, and supernova explosions (Elmegreen & Thomasson 1993), which could result in larger H I velocity dispersions within the optical disks of galaxies with active star formation. The global velocity dispersion of cold gas in models of the Galactic ISM

increases as a function of energy injection rate from stellar winds and/or supernovae (Rosen & Bregman 1995).

High-velocity material could lie "between the horns" of the filled-aperture H I profiles of galaxies, resulting in single-dish spectra without high-velocity wings for galaxies that do have high-velocity gas. If this occurs, the conclusion that galaxies without active star formation lack high-velocity clouds (Schulman *et al.* 1994) would be premature. This is important because the presence of active star formation is the only galaxian property that has compelling evidence for a link to the presence of high-velocity neutral hydrogen in the Arecibo observations. Because the distribution and kinematics of neutral hydrogen in galaxies are inherently complex, it is important to be sure that any H I that appears to be HVCs in external galaxies is not due to warped and flared disks or to inherent asymmetries in the distribution of neutral hydrogen. It is therefore necessary to test the process of modeling spiral galaxies that is used to determine the amount of HVCs in galaxies that have high-velocity wings. These issues can be addressed through VLA observations of a galaxy in the Arecibo sample that does not have high-velocity wings.

This paper reports on sensitive 21 cm observations of UGC 12732 obtained with the VLA for comparison with earlier observations of NGC 5668. Table 1 lists some general information about UGC 12732. The high-sensitivity Arecibo spectrum of UGC 12732 shows no detected high-velocity wings (see Figs. 11(a) and 11(b)), suggesting that this galaxy does not have a disk-wide population of high-velocity clouds (HVCs). The star formation rate in UGC 12732 is an order of magnitude lower than that of NGC 5668, although the galaxies have similar neutral hydrogen masses and sizes. UGC

TABLE 2. Observational setup.

Parameter	Value	
Object	UGC 12732	
Instrument	Very Large Array (VLA)	
Configuration	D Array	
Total observing time	3×7.5 hours + 1×2.5 hours	
Observation dates (1992)	14 Aug 15 Aug 17 Aug 23 Sep	
Time on source (hours)	5.7 2.9 4.4 1.7	
Average number of antennas	26 21 20 26	
	α (B1950.0)	δ (B1950.0)
Field center	$23^h\,38^m\,00^s$	$+25°\,57'\,00''$
Flux density calibrator	3C48	
Phase calibrator	PKS B2251+244	
Central velocity of spectral band	750 km s^{-1}	
Observed baselines (min-max)	35 m $-$ 1030 m	
FWHP of primary beam	32'	
System temperature	60 K	
Total bandwidth	3.125 MHz	652 km s^{-1}
Number of channels	64 (Hanning smoothing applied)	
Channel spacing	10.3 km s^{-1}	
FWHM velocity resolution	10.3 km s^{-1}	
Type of weighting applied to uv–data	natural	uniform
FWHP of synthesized beam	$55'' \times 54''$	$31'' \times 31''$
	5.3 kpc $\times$ 5.2 kpc	3.0 kpc $\times$ 3.0 kpc
RMS noise per channel	0.30 mJy beam^{-1}	0.45 mJy beam^{-1}
Conversion factor T_B(K)/S(mJy)	0.20	0.63
RMS column density of integrated HI map	3.4×10^{18} cm^{-2}	1.6×10^{19} cm^{-2}

12732 does have a smaller optical size than NGC 5668 and a larger H I size to optical size ratio than most galaxies ($R_{\rm H,max}/R_{25}=3.5$, while Salpeter & Hoffman 1996 found a mean of $R_{\rm H,max}/R_{25}=2.7$ for 107 Sdm, Sm, Im, and BCD galaxies). This may indicate that star formation has been less efficient in UGC 12732 than in most late-type spirals. UGC 12732 does not have a larger H I mass fraction within the Arecibo beam when compared to galaxies of similar type; the correction from Arecibo H I flux density to ''true'' H I flux density used by Hewitt *et al.* (1983) gives $M_{\rm H\,I}/M_{\rm T}= 0.14$ for UGC 12732, while Roberts & Haynes (1994) find a median of $M_{\rm H\,I}/M_{\rm T}= 0.15$ for 490 Sm and Im galaxies from the UGC catalog (Nilson 1973). The ''true'' H I flux density is less than the VLA H I flux density because Hewitt *et al.* (1983) assumed a constant H I-to-optical size; the scatter in this parameter is very large, and about 10% of the galaxies they mapped had H I-to-optical sizes larger than that of UGC 12732 (see their Fig. 8).

The VLA observations of UGC 12732 are presented in Sec. 2, a determination of the H I distribution and kinematics is made in Sec. 3, and a discussion of the results and conclusions can be found in Sec. 4. The distance to UGC 12732 is assumed to be 20 Mpc, consistent with $H_0= 50$ km s^{-1} Mpc^{-1} as used in our previous papers.

2. 21 CM OBSERVATIONS

2.1 Data Acquisition

The 21 cm observations presented here were obtained with the VLA in 1992 August and September; the observa-tional configuration is listed in Table 2. The bandwidth used was 3.125 MHz, centered on a heliocentric velocity of 750 km s^{-1} and divided into 64 channels, each covering 10.3 km s^{-1}. The data were taken in 3×7.5 hours plus an additional 2.5 hours that were allocated to make up for data lost during the first three nights of observing. Of these 25 hours, 19 were spent observing UGC 12732. The flux/bandpass calibrator, 3C 48 (flux density = 16.08 Jy at 1417 MHz), was observed for about 8 minutes at the beginning and end of each obser-vation. The phase calibrator, PKS B2251+244 (flux density =1.9 Jy at 1417 MHz), was observed for 3 to 4 minutes every 45 minutes. Due to the many problems that occurred during the data acquisition, only 15 hours of observations of UGC 12732 contained usable data. There were an average of 23 antennas that could be used during this time. A more detailed discussion of the data acquisition problems can be found in Schulman (1995).

2.2 Data Reduction

Data calibration and reduction was performed using the NRAO Astronomical Imaging Processing System (AIPS), following standard procedures. Both polarizations were ex-amined and edited for bad data and amplitude and phase calibrations were done, after which the data were bandpass calibrated. In the following section, the AIPS tasks that were used will be listed in parenthesis.

Two kinds of weighting were used in the data reduction. To optimize the sensitivity to weak, extended H I emission, the Fourier transformation was carried out using a natural

(a)
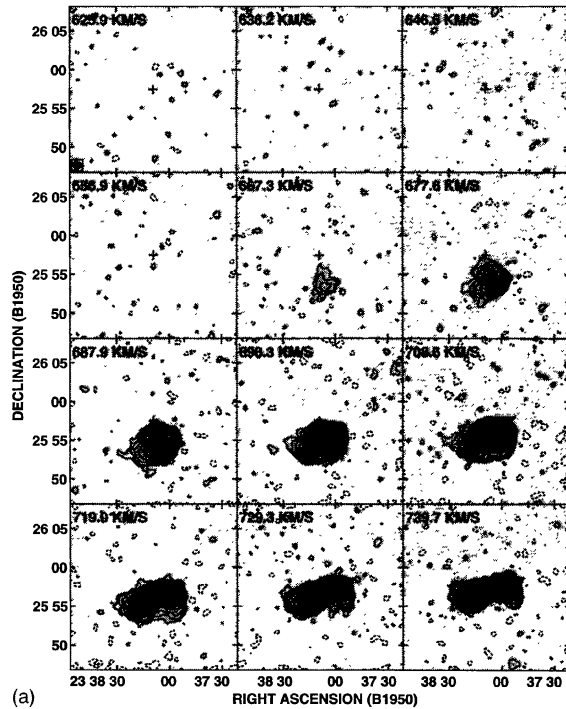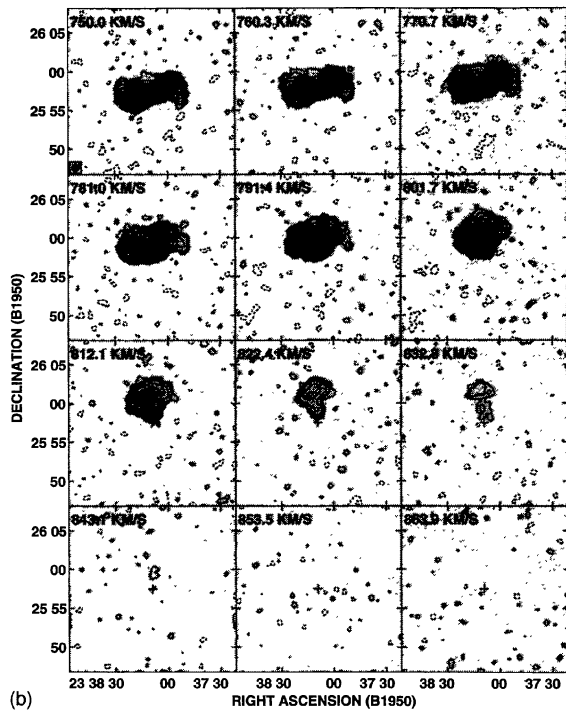
FIG. 1. Naturally-weighted H I channel maps of UGC 12732. The heliocentric radial velocities are indicated in the upper left hand corner of each map, the optical center of the galaxy is indicated with a cross and the FWHP beam is plotted in the lower left hand corner of the first channel. The contours are at −1.5, −0.75, 0.75, 1.5, 3, 6, 12, 24, and 48 mJy beam^{-1} (negative contours are dashed).

(b)

FIG. 2. Naturally-weighted total intensity H I contours of UGC 12732 (the contours are at $N_{H I}$ = 2, 4, 8, 16, 32, 48, 64, 80, and 96×10^{19} atoms cm^{-2}), superposed over a broad-band R image obtained at MDM Observatory. Note that the H I extends well beyond the optical disk of the galaxy. The 3σ rms surface brightness limit is about 25 mag arcsec^{-2}, the optical diameter at 25 mag arcsec^{-2} is about 3′, and the H I diameter at 10^{19} atoms cm^{-2} is 11′.6. The VLA FWHP beam is plotted in the lower right corner.

weighting for the data such that each visibility cell in the uv-plane was weighted according to the integration time. The short spacings are emphasized more than the larger baselines since the uv-tracks are more densely sampled near the center

of the uv-plane. In order to make maps that emphasize emission structures on a smaller scale, the Fourier transformation was carried out using a uniform weighting for the data such that each visibility cell in the uv-plane received equal weight, regardless of the integration time invested in it. Since the primary purpose of this project is the search for weak high-velocity features, the naturally-weighted maps will be emphasized here, but the uniformly-weighted maps are useful in showing that the neutral hydrogen is not smoothly distributed at large column densities in UGC 12732.

Before combining the four nights of observations, a strong (~7 Jy) continuum source located about a degree to the northwest of UGC 12732 had to be subtracted from the data. This source, 3C 465, is associated with NGC 7720, the cD galaxy in Abell 2634 (v =9150 km s^{-1}; Pinkney *et al.* 1993). The area around the source in the August 14 observation was CLEANed (Högbom 1974; Clark 1980) and the resulting clean components were subtracted in the uv-plane from each of the four nights of data (UVSUB). The four nights of data were combined in the uv-plane (DBCON) and preliminary data cubes of both weightings were made (HORUS). The first three and last seven channels in frequency were discarded because the low gain at frequencies near the edge of the bandpass produces a large rms noise. The channels with 502≤v≤626 km s^{-1} and 864≤ v≤1040 km s^{-1} were determined to be line-free, and these channels determined the continuum that was subtracted in the uv-plane (UVLIN; Cornwell *et al.* 1992). Data cubes were made and CLEANed
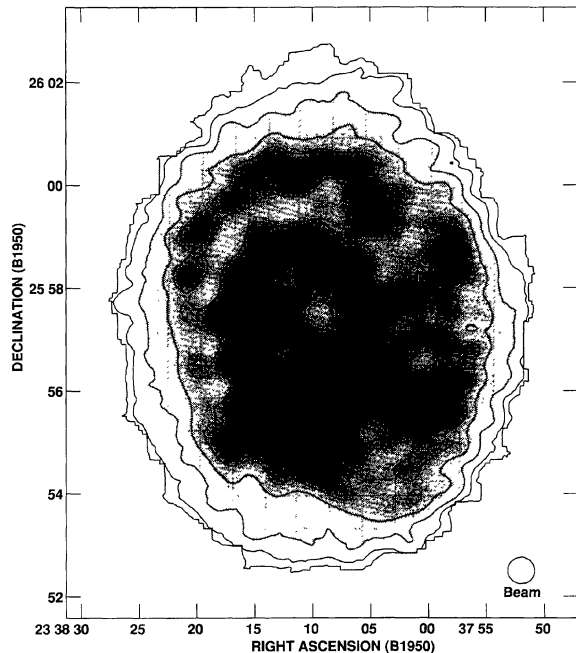
FIG. 3. Uniformly-weighted total intensity H I greyscale and contours of UGC 12732 (the contours are at $N_{H_I} = 4$, 8, 16, 32, 48, 64, 80, 96, and 112×10^{19} atoms cm^{-2}). The FWHP beam is plotted in the lower right corner.
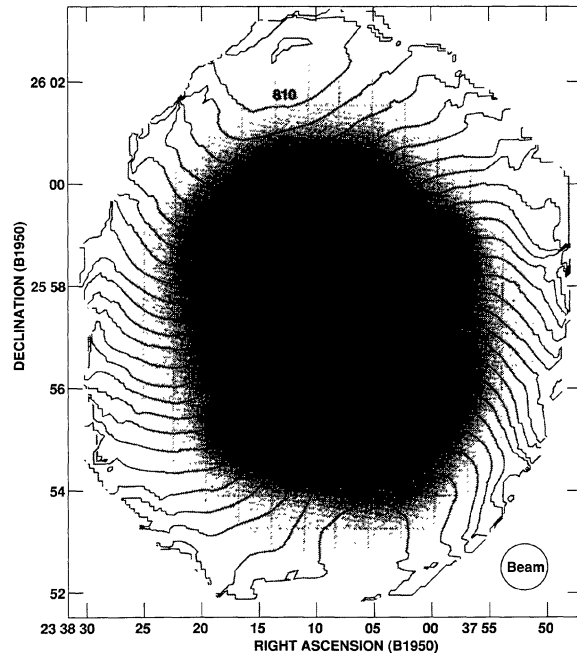

FIG. 4. The intensity-weighted mean velocity field of UGC 12732 (contours; natural weighting) superposed over the naturally-weighted total intensity H I distribution (greyscale). There are contours every 5 km s^{-1} in heliocentric radial velocity from 690 km s^{-1} to 815 km s^{-1}, the systemic velocity is 749 km s^{-1}, and larger velocities are to the north (the contours at 695 km s^{-1} and 810 km s^{-1} are indicated on the map). The FWHP beam is plotted in the lower right corner, and the FWHM velocity resolution is 10.3 km s^{-1}.

(MX). The uniformly-weighted CLEANed channel maps have a nearly uniform sensitivity $\sigma \sim 0.45$ mJy beam^{-1} with a beam size (FWHP) of 31″, while the naturally-weighted CLEANed channel maps have a nearly uniform sensitivity $\sigma \sim 0.3$ mJy beam^{-1} with a beam size (FWHP) of 54″; the sensitivity of both cubes is comparable to the theoretical values. The naturally-weighted channel maps are shown in Fig. 1.

In order to create useful moment maps, it is necessary to eliminate as much noise as possible from the image cubes. The cubes were blanked at the $+2.5\ \sigma$ level (i.e., all pixels with flux densities less than 0.75 mJy beam^{-1} in the naturally-weighted cube were excluded), after which all features that did not occur in at least two adjacent velocity channels were ignored. Moment maps were then created (XMOM). The integrated H I distribution (0th moment; Fig. 2) shows that the neutral hydrogen is much more extended than the optical[5] emission in UGC 12732. The 3σ rms surface brightness limit is about 25 mag arcsec^{-2}, the optical diameter at 25 mag arcsec^{-2} is about 3′, and the H I diameter at 10^{19} atoms cm^{-2} is 11′.6. The galaxy is relatively regular at low neutral hydrogen column densities, but has structure at larger column densities that is most easily visible in the uniformly-weighted map (Fig. 3). This structure includes possible spiral arms (although the optical emission from these arms is very

faint) and a central hole in the H I distribution. The total H I mass is $7.2 \times 10^9\ M_\odot$; the H I mass within the Arecibo beam (see Sec. 4) is $2.2 \times 10^9\ M_\odot$, very similar to the mass of $2.0 \times 10^9\ M_\odot$ determined from the Arecibo observations of Schulman *et al.* (1994). The velocity field (1st moment; Fig. 4) has slightly twisted isovelocity contours outside of the optical radius, indicating that the galaxy has a kinematic warp.

The naturally-weighted, CLEANed cube was rotated by 15° to align the major axis with the pixel grid, after which the cube was transposed so as to obtain a cube in (position along major axis)-(velocity)-(position along minor axis). The position-velocity diagram along the major axis (Fig. 5) shows that the H I velocity dispersion is roughly constant with radius, and that there is little or no high-velocity neutral hydrogen in the galaxy. Such material would be farther than 40–50 km s^{-1} away from the local rotational velocity.

3. NEUTRAL HYDROGEN KINEMATICS AND DYNAMICS

3.1 Fitting the Velocity Field

Tilted rings fitted to the velocity field using the task ROT-CUR (Begeman 1989) in the Groningen Image Processing System (GIPSY) were used to study the kinematics of the neutral hydrogen in UGC 12732. This task derives the rotational velocity (v_{rot}), inclination (i), and position angle (PA) of the galaxy as a function of radius. After the systemic velocity and central position of the galaxy were determined,

---

[5]The *R*-band observations shown here were obtained with the MDM 1.3 m telescope on 1992 October 25 under non-photometric conditions. Photometric images of UGC 12732 obtained in 1993 (Schulman 1995) do not go as deep as these non-photometric observations, and so are not presented here. MDM Observatory is operated by the University of Michigan, Dartmouth College, and the Massachusetts Institute of Technology.
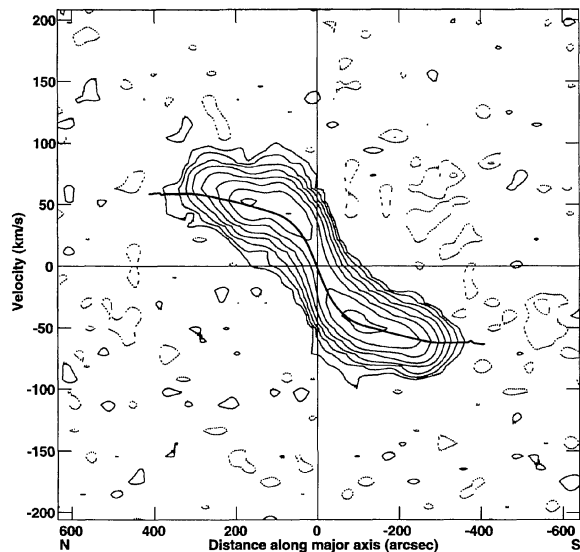
FIG. 5. A position-velocity diagram taken along the major axis of UGC 12732 through the naturally weighted data cube. The rotation curve is indicated by the solid line, and the contours are at -1, -0.5, 0.5, 1, 2, 4, 8, 16, 32, and 64 mJy beam^{-1} (negative contours are dashed).

$v_{\rm rot}$, i, and PA were derived in an iterative fashion for the entire galaxy, keeping all but one parameter fixed for each run. The final values are shown in Fig. 6 and in Table 3. The approaching and receding sides of the galaxy were also fit separately with ROTCUR (the inputs were the solid lines in Fig. 6). Such fits allow an estimate of the errors in the solution to be made, although true asymmetries in the neutral hydrogen distribution appear as well. For clarity of presentation in Figs. 6 and 7, the radii of the rings to be fitted were shifted by 5″ (positive for the receding, negative for the approaching side of the galaxy). Although the convention is to fit both sides of a galaxy at the same radius and then to shift the plotted points, the results of this method were misleading. Note that due to beam smearing the observed values of $v_{\rm rot}$, i, and PA need to be corrected in order to obtain the intrinsic values (the dotted lines in Fig. 6 denote $v_{\rm rot}$ and i after correcting for beam smearing, as do the ''model galaxy inputs'' in Table 3; see below).
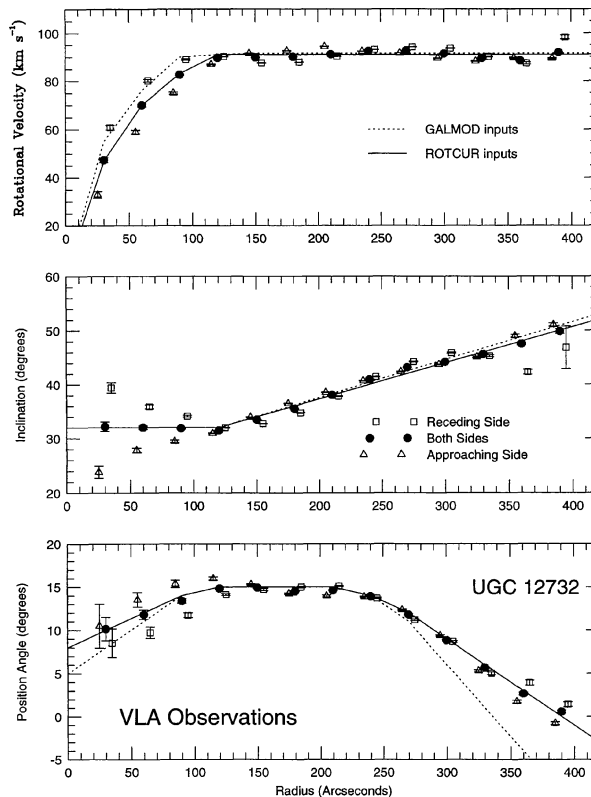

FIG. 6. Tilted-ring (ROTCUR) fits to the velocity field of UGC 12732, showing $v_{\rm rot}$, i, and PA for each 30″ ring. The *solid lines* show the inputs to ROTCUR, the *dotted lines* show $v_{\rm rot}$, i, and PA after correcting for beam smearing (these are the inputs to GALMOD); the symbols are the output from ROTCUR fits to the galaxy (*filled circles* are from fits to the entire velocity field, *open triangles* are from fits to the approaching side of the galaxy, and *open squares* are from fits to the receding side of the galaxy). See text for details.

3.2 Modeling UGC 12732

In order to search for high-velocity material at low column densities, a model galaxy was created that could be compared to the observations of UGC 12732. This model galaxy can account for apparent high-velocity gas due to a warped H I disk, and can also include gas with different ve-

TABLE 3. Results of tilted ring and model galaxy analysis.

| Radius	Tilted ring output			Model galaxy inputs[a]		
	$v_{\rm rot}$	i	PA	$v_{\rm rot}$	i	PA
30″	45.4 ± 0.7 km s^{-1}	$30\overset{\circ}{.}6 \pm 0\overset{\circ}{.}6$	$10\overset{\circ}{.}9 \pm 1\overset{\circ}{.}0$	55 km s^{-1}	32°	8°
60	70.0 ± 0.3	32.0 ± 0.2	12.2 ± 0.3	76	32	11
90	83.3 ± 0.2	32.1 ± 0.1	13.7 ± 0.1	90	32	14
120	90.0 ± 0.1	31.6 ± 0.1	14.7 ± 0.1	91	32	15
150	90.4 ± 0.1	33.7 ± 0.1	14.9 ± 0.1	92	34	15
180	90.8 ± 0.1	35.9 ± 0.1	14.8 ± 0.1	92	36	15
210	90.7 ± 0.1	37.9 ± 0.1	14.4 ± 0.1	92	38	15
240	90.7 ± 0.1	39.9 ± 0.1	13.3 ± 0.1	92	40	14
270	90.8 ± 0.1	42.0 ± 0.1	11.4 ± 0.1	92	43	11
300	91.0 ± 0.1	43.8 ± 0.1	8.6 ± 0.1	92	45	6
330	91.3 ± 0.1	45.9 ± 0.1	6.0 ± 0.1	92	49	1
360	91.9 ± 0.1	47.7 ± 0.1	3.6 ± 0.1	92	51	-4
390	93.0 ± 0.2	50.0 ± 0.2	0.0 ± 0.1	92	53	-9

[a]These values have effectively been corrected for beam-smearing.
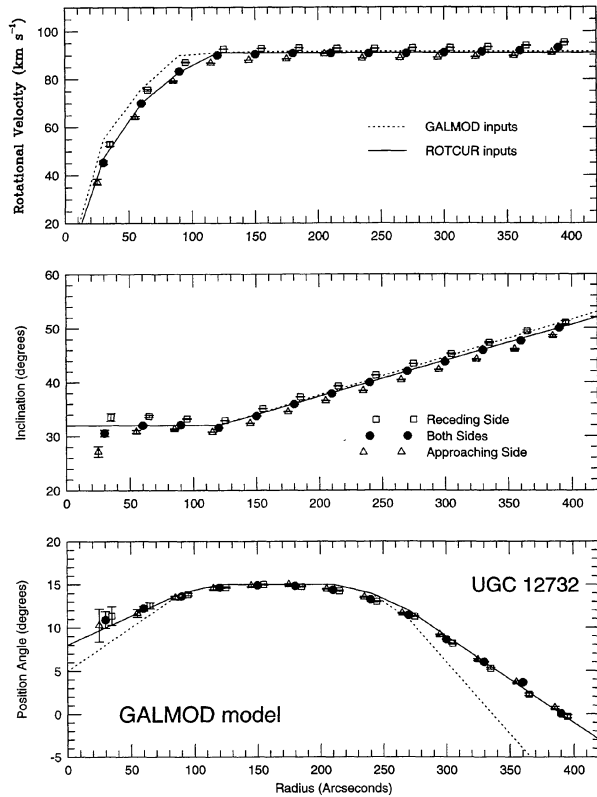
FIG. 7. Tilted-ring (ROTCUR) fits to the velocity field of the GALMOD model of UGC 12732, showing v_{rot}, i, and PA for each 30″ tilted ring. The *solid lines* show the inputs to ROTCUR, the *dotted lines* show the v_{rot}, i, and PA after correcting for beam smearing (these are the inputs to GALMOD); the symbols are the output from the ROTCUR fits to the model galaxy (*filled circles* are from fits to the entire velocity field, *open triangles* are from fits to the approaching side of the model galaxy, and *open squares* are from fits to the receding side of the model galaxy). See text for details.
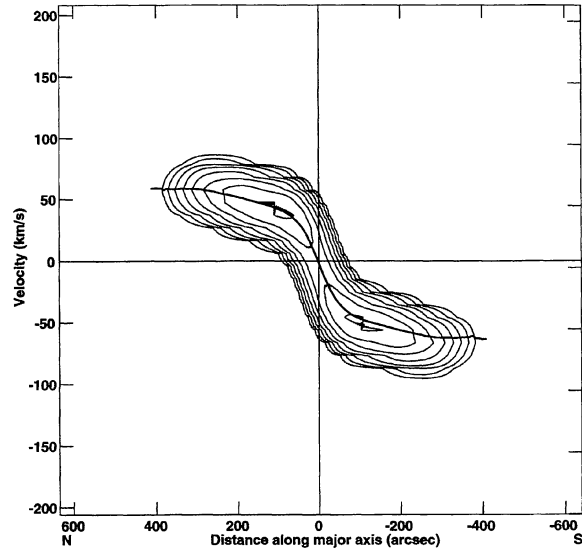

FIG. 8. A position-velocity diagram taken along the major axis of the GALMOD model of UGC 12732. The rotation curve is indicated by the solid line, and the contours are at 0.5, 1, 2, 4, 8, 16, 32, and 64 mJy beam^{-1}. Note the similarity to the observations (Fig. 5).

adjusted until the output H I column density distribution matched that of the azimuthally averaged observations. Initial guesses for the rotational velocity, inclination, and position angle as a function of radius were taken from the tilted-ring (ROTCUR) fits to the observed velocity field (Fig. 6). Since these parameters are beamwidth-smeared, the model galaxy inputs were adjusted until the tilted-ring (ROTCUR) fits to the model matched the fits to the observations. The major

locity dispersions at different radii. The model was constructed using the GIPSY task GALMOD; it consists of neutral hydrogen in circular orbits on rings of different radii and is convolved with the VLA synthesized beam for comparison with the VLA observations. Each ring is characterized by a velocity dispersion, a scale height perpendicular to the plane of the ring, a rotational velocity, an inclination, a position angle, and a column density. The central ''ring'' is actually a disk with a radius of 30″. All rings share the same systemic velocity and central position. A constant velocity dispersion of 9 ± 1 km s^{-1} fits the observations of UGC 12732; the uncertainty in the velocity dispersion comes primarily from the velocity (σ_v=4.4 km s^{-1}) and spatial (θ_{FWHP}= 5.3 kpc) resolution of the observations. The scale height for the H I was assumed to be constant within 12.5 kpc of the center and to increase linearly with radius at larger distances from the center, as is true for our Galaxy (Kulkarni *et al.* 1982) and for M31 (Brinks & Burton 1984); the models are not very sensitive to the scale height of the gas. A disk scale length was not assumed; instead, the initial H I column density as a function of radius was determined by fitting ellipses to the total intensity map (Fig. 2) and correcting for the inclination of the galaxy. The input H I column density distribution was
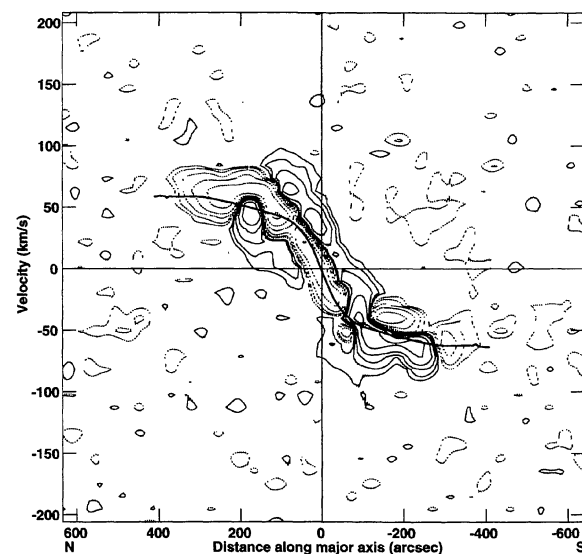

FIG. 9. Residual position-velocity diagram along the major axis of UGC 12732, obtained by subtracting Fig. 8 from Fig. 5. The rotation curve is indicated by the solid line, and the contours are at -16, -8, -4, -2, -1, -0.5, 0.5, 1, 2, 4, and 8 mJy beam^{-1} (negative contours are dashed). High-velocity gas would appear as material at velocities greater than 40 to 50 km s^{-1} with respect to the local rotational velocity; there is no significant high-velocity material present.
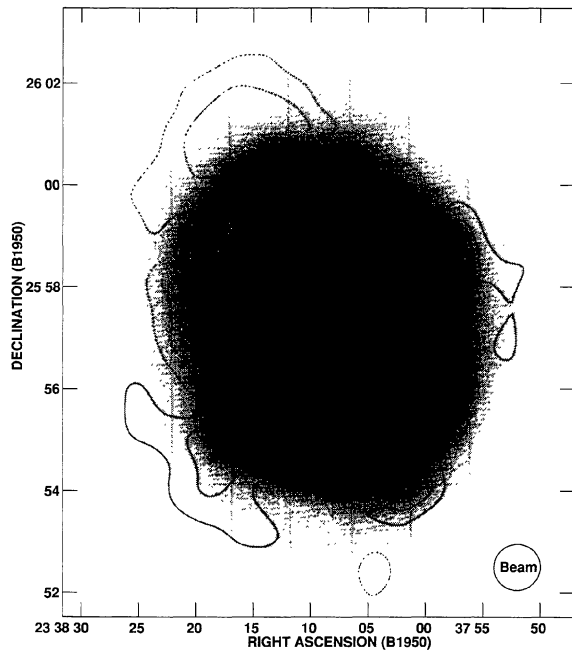
FIG. 10. Residual total intensity H I map of UGC 12732 (the contours are at $N_{H I} = -16,-8,-4,4,8,16$ and 32×10^{19} atoms cm^{-2} with negative contours dashed), superposed over the observed total intensity H I map. The model is azimuthally symmetric while the real galaxy is not, leading to the residuals, which are positive if the observed integrated flux density is larger than the model integrated flux density. The H I FWHP beam is plotted in the lower right hand corner.

modifications were an increased input rotational velocity from 0″to 90″ and steeper changes in position angle with radius between 0″to 90″and at radii larger than 240″. The rotational velocity, inclination, and position angle of the model are shown in Fig. 7 with the model galaxy (GALMOD) inputs shown as dotted lines; these inputs are also presented in Table 3.

The position-velocity diagram along the major axis of the GALMOD model is shown in Fig. 8, and is very similar to that of the VLA observations (Fig. 5). The difference between the galaxy and the model is shown in Fig. 9; the residuals are typically 25% of the observations. The residual total intensity contours, shown in Fig. 10 superposed over the observed total intensity image, are dominated by two features: a region in the south in which the column densities in the galaxy are larger than the column densities in the model, and a region in the north in which the column densities in the galaxy are smaller than the column densities in the model. These azimuthal asymmetries can be seen in Fig. 3. The mean of the absolute value of the ratio of the residual emission to the observed emission is 12%±9%; the maximum residual-to-observed ratio is 38%. Note that the goal of this paper is not to make a model that will match the observations perfectly, but rather to use a relatively simple model to aid in the search for high-velocity neutral hydrogen. We searched for emission that is farther than 40–50 km s^{-1} away from the local rotational velocity in position-velocity space, and set an upper limit of $2 \times 10^7 M_\odot$ to the mass in such high-velocity neutral hydrogen. This corresponds to less than 0.3% of the total amount of neutral hydrogen in UGC 12732. The sensi-
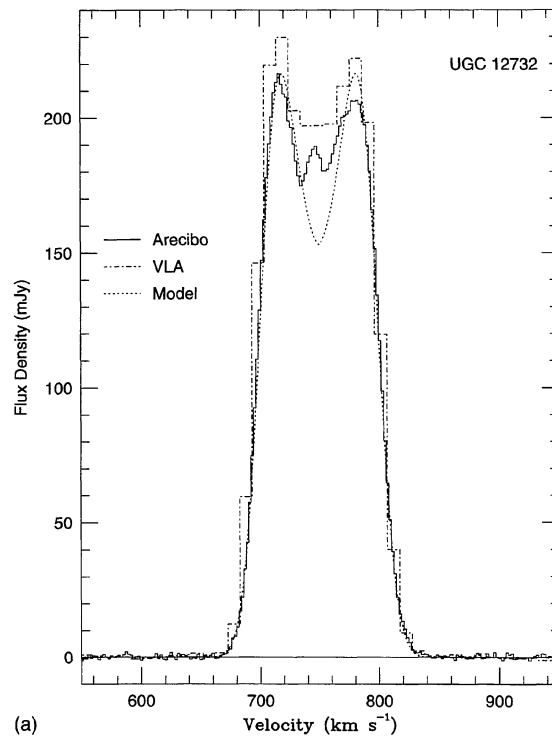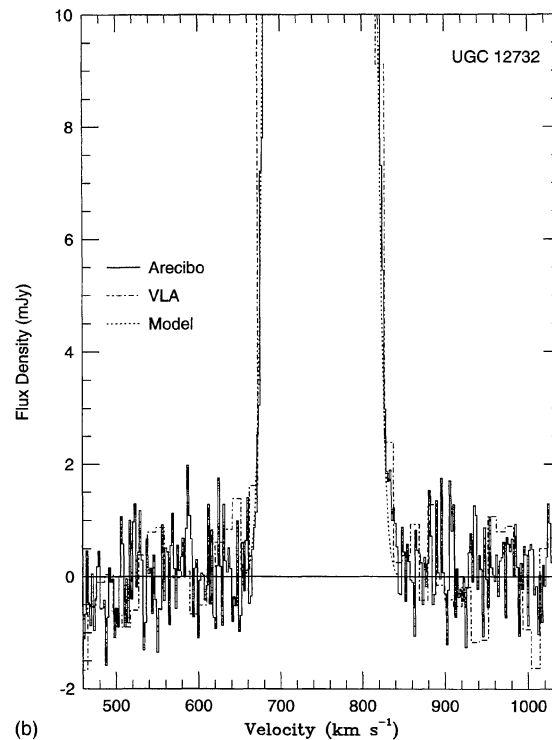
FIG. 11. The H I profile of UGC 12732. The Arecibo spectrum has 2 km s^{-1} channels (*solid histogram*) and the VLA spectrum (*dash-dot histogram*) has 10 km s^{-1} channels. The VLA data were convolved with the Arecibo beam for comparison with the Arecibo spectrum. A spectrum for a disk galaxy model with no high-velocity gas (Schulman *et al.* 1994) is also plotted (*dotted line*). High-velocity gas would appear as wings beyond the model (*dotted line*) spectrum (see Schulman *et al.* 1994 for details). (a) Full flux-density range. (b) Expanded *y-axis*.

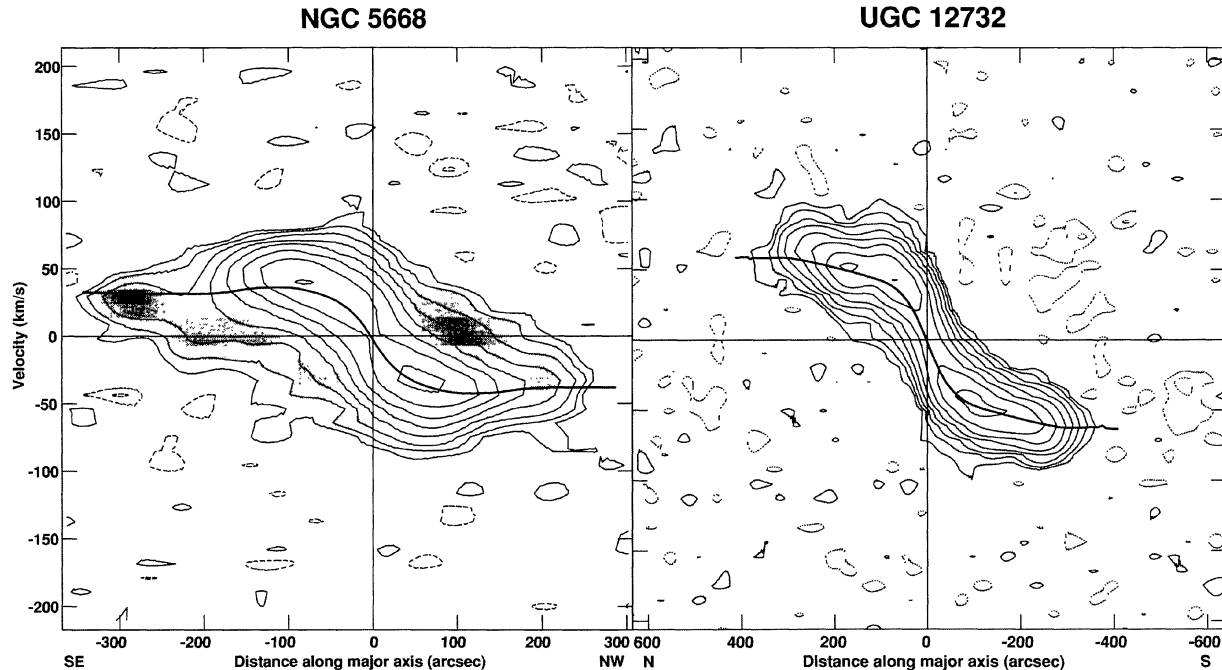**NGC 5668**   **UGC 12732**

FIG. 12. Position-velocity diagrams taken along the major axes of NGC 5668 and UGC 12732. The rotation curves are indicated by solid lines and negative contours are dashed. The contours for NGC 5668 (Fig. 4 from Schulman *et al.* 1996) are at -1.3, -0.65, 0.65, 1.3, 2.6, 5.2, 10.4, 20.8, 41.6, and 83.2 mJy beam^{-1}, while the contours for UGC 12732 (Fig. 5 from this paper) are at -1, -0.5, 0.5, 1, 2, 4, 8, 16, 32, and 64 mJy beam^{-1}. The greyscale indicates the intensity of kinematically distinct neutral hydrogen in NGC 5668 (see Schulman *et al.* 1996 for details).

tivity of these observations to high-velocity gas depends on its spatial and velocity distribution; we would have detected high-velocity H I in UGC 12732 if it had surface densities of a few $\times 10^{19}$ atoms cm^{-2}.

4. DISCUSSION AND CONCLUSIONS

In order to compare the VLA and Arecibo data, the VLA observations were multiplied with the beam shape of the Arecibo 21 cm dual circular feed. The Arecibo beam can be approximated by a Gaussian of FWHP=3.3 plus a 10% sidelobe ring with radii of 276″ and 360″ (Haynes & Giovanelli 1984). The VLA observations recover the H I flux density and the spectral shape observed with the Arecibo telescope (Fig. 11), and so confirm the Arecibo results that there is no evidence for high-velocity wings in the spectrum of UGC 12732 (Schulman *et al.* 1994). Moreover, the VLA data show that there is no high-velocity H I hidden "between the horns," i.e., there is no H I which has a velocity that does not agree with that expected for its location in the disk based on galactic rotation while staying within the same velocity as the bulk of the H I emission. This result is important because the presence of high-velocity clouds as indicated by wings to a single dish spectrum appears to be correlated with active star formation (Schulman *et al.* 1994; Schulman 1995). UGC 12732 has low far-infrared (Schulman *et al.* 1994; Schulman 1995) and Hα (Schulman 1995) luminosities, implying a low star formation rate.

The sample galaxies were selected on the basis of not having nearby companions, but it is difficult to find a truly isolated galaxy. There are galaxies with velocity differences

of less than 300 km s^{-1} and projected distances of less than 400 kpc from half of the galaxies in the sample. Based on our Arecibo sample, galaxies with and without high-velocity H I wings are equally likely to be isolated. NGC 7741, an Scd galaxy 45′ (260 kpc for D=20 Mpc) away from UGC 12732, was visible in the VLA observations, although the H I emission was very weak because the galaxy was well outside the 32′ FWHP primary beam. The systemic velocity of NGC 7741 is within 10 km s^{-1} of that of UGC 12732, implying that the galaxies are spatially close. Despite this possible proximity, neither galaxy appears disturbed in H I or optical observations. The fact that no high-velocity gas was detected suggests that these galaxies have not interacted in the recent past, and it is possible that they have not yet encountered each other.

These VLA observations and GALMOD models confirm that not all disk galaxies have high-velocity clouds of neutral hydrogen. The model of a rotating disk of neutral hydrogen with a velocity dispersion of 9 km s^{-1} throughout adequately reproduces the observations. The residuals left after the model is subtracted from the galaxy are substantial, but are not suggestive of an interaction or of an additional component of neutral hydrogen with a large velocity dispersion.

VLA observations of UGC 12732 and NGC 5668 confirm the Arecibo telescope observations of these two galaxies. In Schulman *et al.* (1996), the galaxy modeling method used here was applied to NGC 5668, which has high-velocity wings that were detected with the Arecibo telescope. A comparison of the position-velocity diagrams along the major axes of these two galaxies (Fig. 12) demonstrates the differences between them. In UGC 12732, the velocity dispersion

is constant with radius, and there is no detected high-velocity emission. NGC 5668, on the other hand, has an abundance of high-velocity neutral hydrogen and a larger H I velocity dispersion within the optical radius. Although the galaxies have similar neutral hydrogen masses and sizes, the star formation rate in NGC 5668 is one to two orders of magnitude greater than the star formation rate in UGC 12732 according to Hα (Schulman 1995) and far-infrared (Schulman *et al.* 1994; Schulman 1995) observations. High-velocity wings were not detected in the four galaxies in the Arecibo survey that have low star formation rates, suggesting a connection between star formation and the presence of high-velocity neutral hydrogen in disk galaxies. The presence of extraplanar diffuse ionized gas (Dettmar 1993; Rand 1996) and extended radio continuum halos (Dahlem *et al.* 1995) are also related to the star formation rate in the disks of spiral galaxies. These results lend support to the hypothesis that at least some high-velocity clouds in disk galaxies are driven into the halo by active star formation, and that when active star formation is absent there is little mass in high-velocity clouds of neutral hydrogen.

REFERENCES

Begeman, K. 1989, A&A, 223, 47

Boulanger, F., & Viallefond, F. 1992, A&A, 266, 37

Bregman, J. N. 1980, ApJ, 236, 577

Brinks, E., & Burton, W. B. 1984, A&A, 141, 195

Centurión, M., Vladilo, G., de Boer, K. S., Herbstmeier, U., & Schwarz, U. J. 1994, A&A, 292, 261

Clark, B. G. 1980, A&A, 89, 377

Cornwell, T. J., Uson, & Haddad, N. 1992, A&A, 258, 583

Dahlem, M., Lisenfeld, U., & Golla, G. 1995, ApJ, 444, 119

Danly, L., Albert, C. E., & Kuntz, K. D. 1993, ApJ, 416, L29

Dettmar, R.-J. 1993, Rev. Mod. Astron., 6, 33

de Vaucouleurs, G., de Vaucouleurs, S., Corwin, H., Buta, R., Paturel, G., & Fouqué, P. 1991, Third Reference Catalogue of Bright Galaxies (Springer, New York)

Dickey, J. M., Hanson, M. M., & Helou, G. 1990, ApJ, 352, 522

Dressel, L. L., & Condon, J. J. 1976 ApJS, 31, 187

Elmegreen, B. G., & Thomasson, M. 1993, A&A, 272, 37

Haynes, M. P., & Giovanelli, R. 1984, AJ, 89, 758

Hewitt, J. N., Haynes, M. P., & Giovanelli, R. 1983, AJ, 88, 272

Högbom, J. A. 1974, A&AS, 15, 417

Kamphuis, J., & Sancisi, R. 1993, A&A, 273, L31

Kulkarni, S. R., Blitz, L., & Heiles, C. 1982, ApJ, 259, L63

Murai, T., & Fujimoto, M. 1980, PASJ, 32, 581

Nilson, P. 1973, Uppsala General Catalogue of Galaxies (Royal Society of Sciences of Uppsala, Uppsala) (UGC)

Pinkney, J., Rhee, G., Burns, J. O., Hill, J. M., Oegerle, W., Batusky, D., & Hintzen, P. 1993, ApJ, 416, 36

Rand, R. J. 1996, in The Interplay Between Massive Star Formation, the ISM, and Galaxy Evolution, edited by D. Kunth, B. Guiderdoni, M. Heydari-Malayeri, and T. X. Thuan (Editions Frontières, Gif-sur-Yvette Cedex), p. 515

Roberts, M. S., & Haynes, M. P. 1994, ARA&A, 32, 115

Rosen, A., & Bregman, J. N. 1995, ApJ, 440, 634

Salpeter, E. E., & Hoffman, G. L. 1996, ApJ, 465, 595

Schulman, E. 1995, Ph.D. thesis, University of Michigan

Schulman, E., Bregman, J. N., Brinks, E., & Roberts, M. S. 1996, AJ, 112, 960

Schulman, E., Bregman, J. N., & Roberts, M. S. 1994, ApJ, 423, 180

Shapiro, P. R., & Field, G. B. 1976, ApJ, 205, 762

Wakker, B. P. 1990, Ph.D. thesis, Groningen University

Wakker, B. P. 1991, A&A, 250, 499

Wakker, B., Howk, C., Schwarz, U., van Woerden, H., Beers, T., Wilhelm, R., Kalberla, P., & Danly, L., 1996, ApJ, 473, 834

Wakker, B. P., van Woerden, H., Schwartz, U. J., Peletier, R. F., & Douglas, N. G. 1996b, A&A, 306, L25